26th International Congress of Mechanical Engineering
November 22-26, 2021, Virtual Congress, Brazil

COB-2021-0978
ACCURACY ANALYSIS OF MULTIBODY SYSTEMS WITH JOINT CLEARANCE IN FOUR-BAR MECHANISMS

Rogério Sales Gonçalves
Glênio Simião Ramalho
School of Mechanical Engineering, Federal University of Uberlândia, Uberlândia - MG, Brazil
rsgoncalves@ufu.br, gleniosimiao@gmail.com

Fabian Andres Lara-Molina
Department of Mechanical Engineering, Federal University of Technology - Paraná, Cornélio Procópio - PR - Brazil
fabianmolina@utfpr.edu.br

Marco Ceccarelli
Department of Industrial Engineering, University of Rome Tor Vergata, Roma, Italy
marco.ceccarelli@uniroma2.it

Abstract. *A multibody system consists on a kinematic chain that is composed of links that can be rigid or flexible, interconnected by joints, in general lower pair such as revolute, prismatic and spherical joints. These joints work properly only if an adequate clearance is ensured. In general, a joint is considered in a design process as ideal i.e., with no clearence in the kinematic pair. When the clearance exists, it can affect the accuracy of the system operation. This paper aims at presenting a numerical approach to obtain the structure displacements that are produced by the stiffness of the structure and the joint clearances. Thus, the joint clearances are included within the model. The compliant displacement of the structure is obtained by a matrix structural analysis (MSA) that considers the compliance of links and joints as is superposed to displacements obtained from joint clearances to obtain the total displacements of the structure. Moreover, the uncertainties of the parameters are modeled as random variables. The compliant displacements in the presence of the uncertainties are obtained by using the Monte Carlo Simulation. The numerical results of simulations are shown for a specific symmetric four-bar linkage as an illustrative example.*

Keywords: *Multibody Systems, Stiffness, Clearance, Simulation, Uncertainties*

1. INTRODUCTION

Multibody systems are kinematic chains of rigid or flexible links connected by joints. As an example of a multibody system, parallel mechanisms have widely been studied in recent years. Despite their potential advantages, parallel mechanisms still present challenging drawbacks that can affect their potential benefits: workspace size, singularities, stiffness, and accuracy (Gonçalves *et al.*, 2009; Gonçalves and Carvalho, 2009; Gosselin *et al.*, 1990).

The accuracy analysis of parallel mechanisms should consider some factors that decrease the positioning accuracy performance. These factors are compliant displacements due to the flexibility of links and joints, positioning errors of active joints, and joint clearances. In particular, the compliant displacements of links, joints, and joint clearance can affect the accuracy of the mechanism. The compliant displacements can be derived from the stiffness study of parallel robotic structures. In this paper, the influent of compliance displacements are found using the Matrix Structural Analysis (MSA) like proposed by Gonçalves (2009).

In general, for modeling multibody systems, joints are considered ideal, i. e., frictionless and without clearance, but in practice, the joints are made with clearances to allow movement between the elements. Nevertheless, it has been demonstrated that small clearance can lead to problems such as vibrations, fatigue, lack of accuracy, and errors in the position and orientation of the mobile platform (Zhang *et al.*, 2014; Lara-Molina *et al.*, 2018). Therefore, when the articulated mechanism requires high accuracy, the clearance can not be ignored (Meng *et al.*, 2009), and a realistic model should include the displacements produced by the flexibility of joints and links and the joints clearance. Additionally, manufacturing errors and assembling tolerances introduce small variations in the geometry of the links that also produce position errors affecting the performance of the system. Thus, the uncertainties and their effects should be evaluated on the performance of the mechanism.

Several research studies have quantified the uncerteinties of multibody systems by considering different approaches. Thus, the probabilistic theory has been used to study the effects of uncertainties on the performance of mechanisms. By using this approach, the uncertainties were modeled as random variables (Lara-Molina *et al.*, 2015; Rao and Bhatti, 2001). Consequently, the reliability associated with the tolerances of geometrical and dynamical parameters of the multibody systems were studied as an extension of this study (Pandey and Zhang, 2012; Lara-Molina and Dumur, 2020). As an alternative approach to the probabilistic approach, the fuzzy theory has been applied to analyze the dynamic behavior of multibody systems (Walz and Hanss, 2013; Lara-Molina and Dumur, 2021).

In this paper, an analytical formulation is proposed for obtaining the structure displacements due to the joint clearance. Thus, the effect of joint clearance was included within the model. The compliant displacement of the structure, obtained by the matrix structural analysis (MSA) that considers the compliance of links and joints, is superposed to displacements obtained from joint clearances to obtain the total displacements of the structure. Moreover, the uncertainties of the parameters were modeled as random variables. The compliant displacements in the presence of the uncertainties were obtained by using the Monte Carlo Simulation. The results of the numerical simulations are computed for a specific symmetric four-bar linkage as an illustrative example and to show the feasibility of the proposed approach.

2. APPROACH FOR ACCURACY ANALYSYS OF MULTIBODY SYSTEMS

This section presents an analytical formulation for obtaining the structure displacements. The uncertainties are included in the parameters that define the stiffness of flexible joints and the joint clearances.

2.1 Compliant Displacement Model of Four-Bar Linkage Mechanisms

In order to explain the proposed methodology, the analysis of the influence of joint clearances and the compliant displacements applied to a four bar linkage mechanism. For the dynamic analysis, the mechanism is considered as composed of rigid links connected by frictionless joints and without clearance. The velocities and accelerations of links can be obtained from the kinematics of the rigid body. The dynamic analysis is performed by using the kinetostatic analysis with the matrix method which considers the free-body diagram of each link of the mechanism and the inertia forces and inertia torque is assumed acting at the center of mass.

The inertia forces, F_{Oj}, and the inertia torque, T_{Oj}, can be given as

$$F_{Oj} = (m_j A_{gj}) e^{i(\beta_j + \pi)} \quad j = 1, \dots n \tag{1}$$

$$T_{Oj} = -I_j \alpha_j \tag{2}$$

where F_{Oj} represents the inertia force acting on a link j, m_j is the mass of a link; β_j defines the direction of the center mass acceleration A_{gj} and n is the number of links. The inertia force has the opposite direction of the center mass acceleration, $(\beta j + \pi)$. I_j is the mass moment of inertia about the center of gravity of the link j and α_j is the angular acceleration of link j. The inertia torque acts in opposite direction to the angular acceleration.

Figure 1 shows a four-bar linkage with inertial forces, accelerations, and velocities at links, and in Fig. 1 is sketched the free-body diagrams where the inertia forces and inertia torques are applied to the link center of mass, where T_L represents a torque due to the external loading on the mechanism.

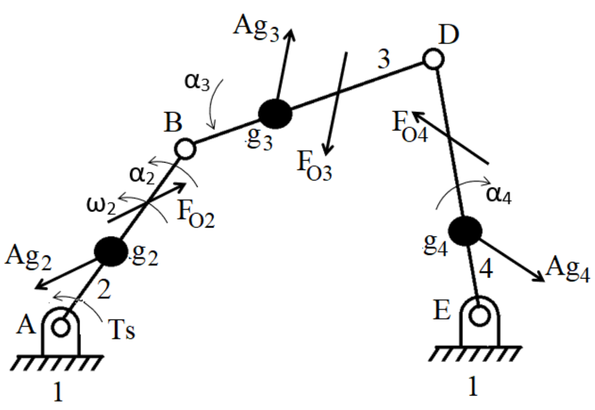

Figure 1. Inertia forces, accelerations and velocities in a four-bar linkage.

From free-body diagram, as shown in Fig. 2, the kinetostatic equations $\sum F_x = 0$, $\sum F_y = 0$ and $\sum T_{Oj} = 0$, can be written in a straightforward way. The unknowns to be determined are the joint reactions F_{12x}, F_{12y}, F_{23x}, F_{23y}, F_{34x}, F_{34y}, F_{14x} and F_{14y} and drive torque T_s. The Newton's third law gives $F_{jkx} = F_{kjx}$. Reorganizing adequately the

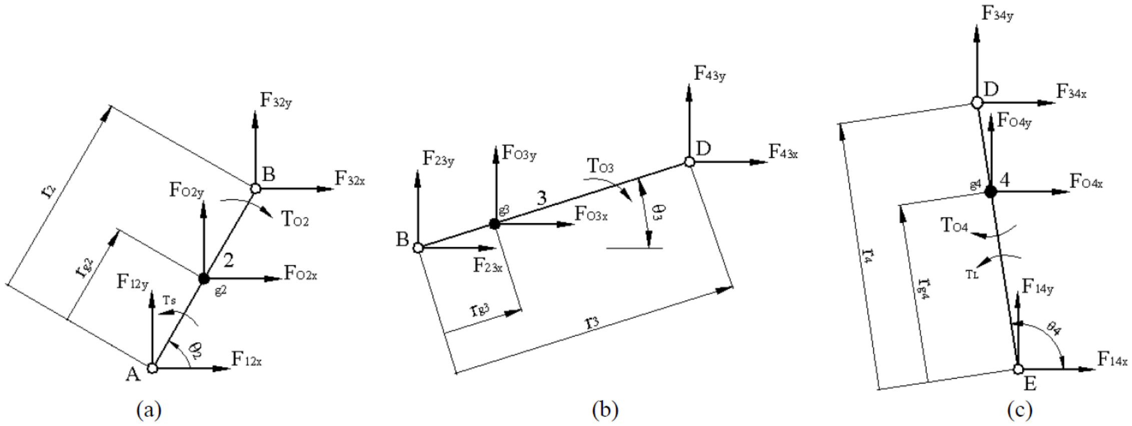

Figure 2. (a), (b) and (c) show free-body diagrams of links used for the kinetostatic equilibrium.

kinetostatic equilibrium equations can be written as

$$
\begin{aligned}
&F_{O2x} = -F_{12x} + F_{23x} \\
&F_{O2y} = -F_{12y} + F_{23y} \\
&T_{O2y} = -F_{12x} r_{g2} \sin(\theta_2) + F_{12y} r_{g2} \cos(\theta_2) - T_s - F_{23x}(r_2 - r_{g2}) \sin(\theta_2) + F_{23y}(r_2 - r_{g2}) \cos(\theta_2) \\
&F_{O3x} + F_y = -F_{23x} + F_{34x} \\
&F_{O3y} = -F_{23y} + F_{34y} \\
&T_{O3} = -F_{23x} r_{g3} \sin(\theta_3) + F_{23y} r_{g3} \cos(\theta_3) - F34x(r_3 - r_{g3}) \sin(\theta_3) + F_{34y}(r_3 - r_{g3}) \cos(\theta_3) \\
&F_{O4x} = -F_{34x} - F_{14x} \\
&F_{O4y} = -F_{34y} - F_{14y} \\
&T_{O4} = F_{34x}(r_4 r_{g4}) \sin(\theta_4) - F_{34y}(r_4 - r_{g4}) \cos(\theta_4) - F_{14x} r_{g4} \sin(\theta_4) + F_{14} r_{g4} \cos(\theta_4) - T_L
\end{aligned}
\tag{3}
$$

The system of equations (3) can be written in a matrix form as

$$
[F_D] = [L][F_B] \tag{4}
$$

where $[F_D]$ is a column vector containing the known values of the inertia forces and torques, $[L]$ is a square matrix containing the length of the links and position angles and $[F_B]$ is a column vector containing the values of unknown reaction forces in the joints and the required drive torque (Gonçalves *et al.*, 2009). Thus, Equation (4) being of linear form can be solved in a closed-form to obtain the reaction forces.

2.2 Stiffness of Links and Joints Modeling

As proposed by Gonçalves (2009) the stiffness of a joint can be expressed as

$$
K_{joint} = \begin{bmatrix} k_c & -k_c \\ -k_c & k_c \end{bmatrix} \tag{5}
$$

where $k_c = diag(k_{tx}, k_{ty}, k_{tz}, k_{rx}, k_{ry}, k_{rz})$; k_{tx}, k_{ty}, k_{tz} are the translation stiffness and k_{rx}, k_{ry}, k_{ry} are the rotational stiffness along the x, y and z axes. The stiffness matrix of the three-dimensional straight bar with a uniform cross-sectional area is given by (Shabana, 2003).

$$
K_j = \begin{bmatrix} k_{bj} & -k_{bj} \\ -k_{bj} & k_{bj} \end{bmatrix} \tag{6}
$$

where k_{bj} can be expressed as

$$K_j = \begin{bmatrix} \frac{A_jE_j}{L_j} & 0 & 0 & 0 & 0 & 0 \\ 0 & \frac{12E_jI_{zj}}{L_j^3} & 0 & 0 & 0 & \frac{6E_jI_{zj}}{L_j^2} \\ 0 & 0 & \frac{12E_jI_{yj}}{L_j^3} & 0 & -\frac{6E_jI_{yj}}{L_j^2} & 0 \\ 0 & 0 & 0 & \frac{G_jJ_j}{L_j} & 0 & 0 \\ 0 & 0 & -\frac{6E_jI_{yj}}{L_j^2} & 0 & \frac{4E_jI_{yj}}{L_j} & 0 \\ 0 & \frac{6E_jI_{zj}}{L_j^2} & 0 & 0 & 0 & \frac{4E_jI_{aj}}{L_j} \end{bmatrix} \tag{7}$$

On Equation (7) E_j and G_j are, respectively, the modulus of elasticity and the shear modulus of element j; I_{yj}, I_{yz} are the moment of areas about the Y and Z axes, respectively. J is the Saint-Venant torsion constant and A_j is the cross-sectional area. For the application of MSA is necessary to write the stiffness matrices of all elements in the same reference frame. This transformation, element by element, must be held before the assembly of the stiffness matrix of the structure. This transformation matrix, T_j, can be obtained from linear algebra. Thus, the stiffness matrix of the elements in a common reference frame (elementary stiffness matrix), for segments, K_j^e , and for joints, K_{joint}^e, can be written as

$$[K_j^e] = [T_j][K_j][T_j]^T \tag{8}$$

$$[K_{joint}^e] = [T_j][K_{joint}][T_j]^T \tag{9}$$

After obtaining the stiffness matrix of each beam and joint in a common reference frame, the stiffness matrix of the whole structure can be obtained using a procedure from MSA. Based on how the structural elements are connected, from their nodes, it is possible to define a connectivity matrix. As each segment and joint stiffness are known, the global stiffness matrix is obtained by a superposition procedure. This global stiffness matrix is singular because the system is free, that is, it has no restrictions. After application of the boundary conditions, for example, where the displacements are known, the new matrix is invertible and the compliant displacements can be computed as

$$\{U\} = K^{-1}\{W\} \tag{10}$$

The procedure is described in detail in (Júnior *et al.*, 2016; Gonçalves *et al.*, 2016).

2.3 Joint Clearances Model

In theoretical multibody models, it is assumed that the connecting points of two bodies, linked by an ideal or perfect revolute joint, are coincident. When a joint clearance is considered these two points can not be coincident. In a revolute joint the difference in radius between the bearing, R_B, and the journal, R_J, defines the radial clearance ϵ which enables a journal motion within the bearing as shown in Fig. 3. Thus, when the clearance is present in a revolute joint, two kinematic constraints are removed and two degrees of freedom are introduced instead.

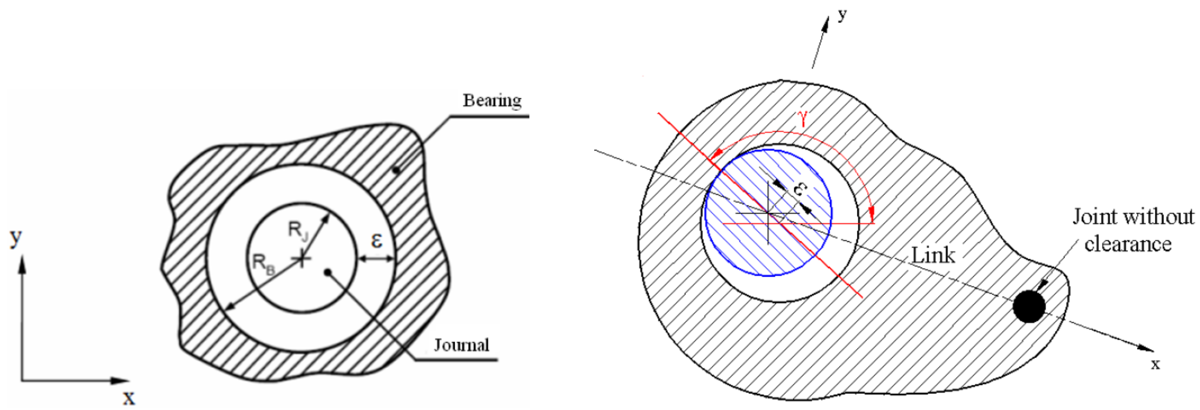

(a) Clearance model. (b) Parameters of the clearance.

Figure 3. Revolute joint with clearance.

In this work, a methodology is proposed for evaluating the influence of the clearance, ϵ, in revolute joints in multibody systems. The joint clearance causes the displacement of the parts that form the joint, Fig. 4a, with infinite places of contact between the two parts. Figure 4b is characterized by the angle γ that is obtained from the dynamic model of the mechanism. Knowing the contact position and the value of the clearance is possible to determine the displacements in the direction of axes x and y, shuch as

$$\begin{aligned} \epsilon_x &= \epsilon \cos(\gamma) \\ \epsilon_y &= \epsilon \sin(\gamma) \end{aligned} \tag{11}$$

From the reallocated position of elements, Fig. 4b, by considering the clearance, the position and orientation of the other elements can be updated in order to determine the influence of the clearance along with the structure.

2.4 Uncertainties Model and Monte Carlo Simulation

Based on the model of the mechanism presented previously, the uncertainties are considered in the following parameters: the stiffness coefficients of the joints ($k_{tx}, k_{ty}, k_{tz}, k_{rx}, k_{ry}, k_{rz}$ of Eq. (5)), the parameters of joint clearances (ϵ and γ of Eq. (11)) and also an external force applied on the mechanism (F_y). Consequently, these parameters can be set on the vector $\mathbf{u} = \begin{bmatrix} k_{tx} & k_{ty} & k_{tz} & k_{rx} & k_{ry} & k_{rz} & \epsilon & \gamma & F_y \end{bmatrix}$. The uncertain paramenters of mechanism are modeled as random variables as proposed in (Lara-Molina *et al.*, 2018). Thus, a single uncertain parameter is defined as

$$u_i(\Omega) = u_i + u_i \delta_u \xi(\Omega) \tag{12}$$

where u_i is the nominal link length, δ_u is the maximum percentual deviation around the nominal link length, and $\xi(\Omega)$ is the unit normal random variable with mean and variance being zero and one, respectively and Ω is a random process. The unit normal random variable is governed by a normal distribution according to the central limit theory (Montgomery and Runger, 2010); that has been conveniently selected in order to evaluate the uncertain parameters.

Moreover, the Monte Carlo simulation (MCS) is used to evaluate the dynamic response of the four-bar linkage based on the matrix structural analysis (MSA). The MCS has three main steps: i) sampling of the uncertain parameters $\mathbf{u}$ to obtain a set of n_s random inputs; ii) the outputs of the system $\{U\}$ (displacements) are computed for each random input. iii) a statical analysis is carried out to find the mean and standard deviation of the output. The algorithm of MCS is presented in Fig. 4.

Initialization;
Sampling of the random inputs: $\mathbf{u}_{n_s}$
for i *to* n_s **do**
  $\{U\}(i) \leftarrow MSA(\mathbf{u}_i)$
  $i \leftarrow i + 1$
end

$$\mu_{\{U\}} \leftarrow \mu(\{U\}_{n_s \times 1}) \tag{13}$$

$$\sigma_{\{U\}} \leftarrow \sigma(\{U\}_{n_s \times 1}) \tag{14}$$

end;

(a) Pseudocode.

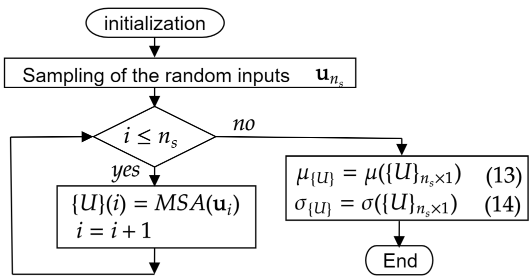

(b) Flowchart.

Figure 4. Monte Carlo simulation to compute the robustness criterion: a) Psudocode, b) Flowchart.

where the operators $\mu(.)$ and $\sigma(.)$ denote the mean and standard deviation, respectively form Eqs. (13) and (14).

3. NUMERICAL RESULTS

In this section, a numerical simulation of asymmetric four-bar linkage was carried out, as shown in Fig. 5a, assuming that an upward external force, Fy, is applied to the center of mass of coupler link 3 and no external torque are applied to the mechanism. The reported simulation refers to a linkage that has the following data: l = 0.1 m; all links have a square cross-section of 0.00635 m $\times$ 0.0127 m. The links were modeled as bars (according to modeling of section 2.2) with a Young modulus E =2$\times$10^{11}N/m^2. The rotational active joint defined by the angle θ was considered as clamped at a fixed position; therefore, the input velocities and accelerations are zero. The rotational passive joints were modeled without rotational stiffness around their rotational axes and clearances (according to section 2.3). The modeling o the four-bar linkage follows the modeling presented in section 2.1. The uncertainties were also included in the model according to the modeling presented in section 2.4. These uncertainties were introduced in the following inputs and parametes: a) external force applied on center of mass of coupler link 3, $F_y(\Omega) = 100N + 5(\Omega)$ N; b) $k_j = 2 \times 10^{11} + 1 \times 10^{10}(\Omega)$N/m stiffness of joints (of Eq. (5)) c)$\epsilon = 1 \times 10^{-3} + 5 \times 10^{-5}(\Omega)$m and $\gamma = 180 + 180(\Omega)^o$ joint clearances. The Monte Carlo simulation of Fig. 4 was worked out $n_s = 100$ samples.

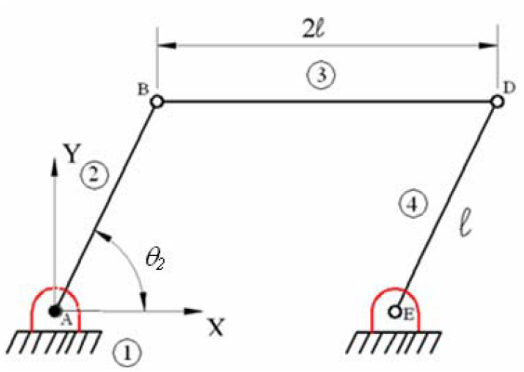

(a) Segments.

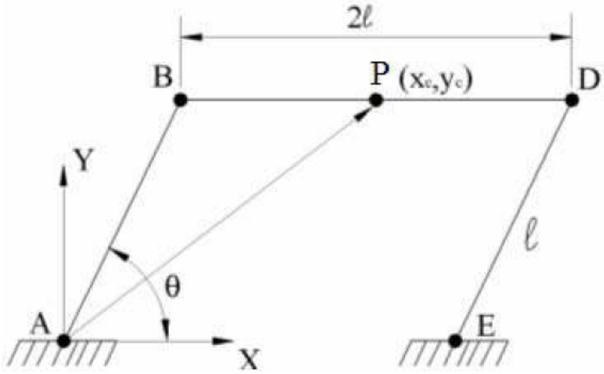

(b) Schematic representation and point P.

Figure 5. Symmetric four-bar linkage.

Based on Fig. 5b, one can write the kinematic equations to describe the positions of the points B, D, and P of the mechanism as a function of the kinematic variable θ, as

$$\begin{aligned}
&x_A = 0; y_A = 0\\
&x_B = l\cos(\theta); y_B = l\sin(\theta)\\
&x_P = l\cos(\theta) + l; y_P = l\sin(\theta)\\
&x_D = x_E + l\cos(\theta); y_D = l\sin(\theta)\\
&x_E = 2l; y_E = 0
\end{aligned} \tag{15}$$

The simulation consists of computing the flexible displacement of point P by using matrix structural analysis (MSA) and the uncertainties.

Table 1 shows computed values of the flexible displacement of the point P along the x and y directions as a function of the kinematic variable θ where $0 \leq \theta \leq 360^o$; μ and σ denote the mean and standard deviation of the point P along x and y axes subject to uncertainties. The flexible displacements obtained at the singular positions are larger than the flexible displacements obtained for other positions and the sigular positions are obtained for $\theta = 0^o$, $\theta = 180^o$, and $\theta = 360^o$. The condition number $\kappa(K)$ of the total stiffness matrix K (see Eq. (10)) was computed in the analysis, where $\kappa(K) = ||K^{-1}||\,||K||$. Moreover, the condition number get also larger values for the singular positions (see Table 1).

Table 1. Computed outputs of displacements of point P.

$\boldsymbol{\theta}[^o]$	**x** [m]	**y** [m]	$\boldsymbol{\mu_x}$ [m]	$\boldsymbol{\mu_y}$ [m]	$\boldsymbol{\sigma_x}$ [m]	$\boldsymbol{\sigma_y}$ [m]	Condition number ($\kappa(K)$)
0	0.2	0	0.1005	0.0002	5.3010×10^6	1.3381×10^8	9.6220×10^{15}
30	0.1866	0.0500	0.0889	0.0003	0.0499	0.0004	5.6899×10^8
60	0.1500	0.0866	0.0536	0.0003	0.0849	0.0003	3.5878×10^8
90	0.1000	0.1000	0.0040	0.0002	0.1002	0.0003	2.9682×10^8
150	0.0134	0.0500	-0.0844	0.0003	0.0529	0.0004	5.4873×10^8
180	0	0	0.0019	0.0012	613794	2.2030×10^7	0.5776×10^{15}
230	0.0357	-0.0766	-0.0635	0.0003	-0.0764	0.0003	5.4659×10^8
300	0.1500	-0.0866	0.0503	0.0003	-0.0864	0.0003	3.8653×10^8
350	0.1985	-0.0174	0.0988	0.0002	-0.0175	0.0004	6.6970×10^8
360	0.2	0	0.1005	0.0002	5.3010×10^6	1.3381×10^8	9.6220×10^{15}

Figure 6 shows the stiffness mapping where the singular positions were excluded. Figure 6a shows the trajectory of point P (ref) without joint clearances and loads applied on the mechanism. Then, the envelope bounded by the limit lines (max and min) indicates the trajectories of point P obtained when the mechanism is subjected to uncertainties in the joint clearances, joint stiffness, and the external force (see Fig. 6a) by using the Monte Carlo simulation; it is observed that the trajectory of point P is contained within the envelope. Additionally, Fig. 6a shows the trajectories (samples) obtained during the execution of the Monte Carlo simulation.

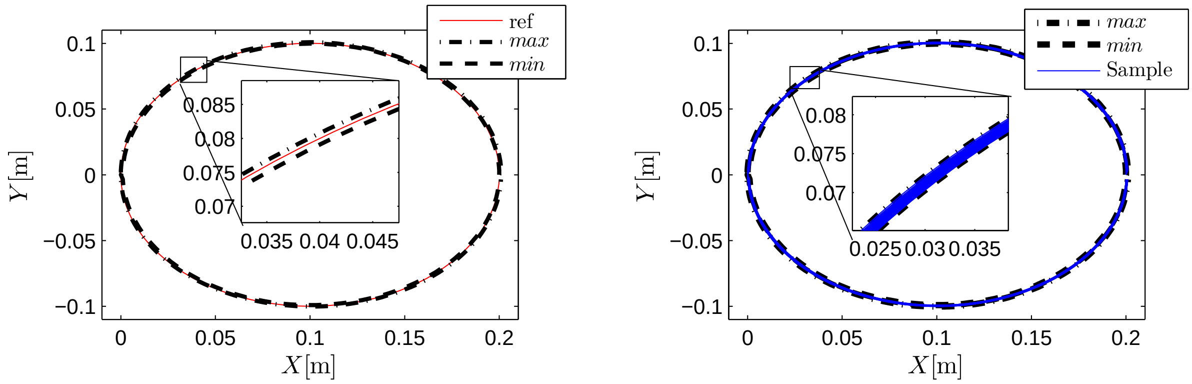

(a) Envelope. (b) Samples.

Figure 6. Simulated computed trajectory of the point P of the symmetric four-bar linkage.

Figure 7 shows the displacement of the point P subjected to uncertainties for $\theta = 30^o$. The histograms of the displacement for the x axis (Fig. 7a) and the y axis (Fig. 7b) are presented; the probability density function (PDF) was approximated by considering a normal distribution. The parameters of the normal distribution (mean (μ) and standard deviation (σ)) for every considered θ are apresentad in Table 1.

The computation of the Monte Carlo simulation demands the solution of the matrix structural analysis (MSA) n_s times as shown in the algorithm of Fig. 4. Therefore, the computation effort increases regarding the matrix structural analysis presented in 62016Júnior *et al.*Júnior, Carvalho and Gonçalves. Nevertheless, the method proposed allows computing the effect of uncertain parameters on the positioning accuracy of the multibody system.

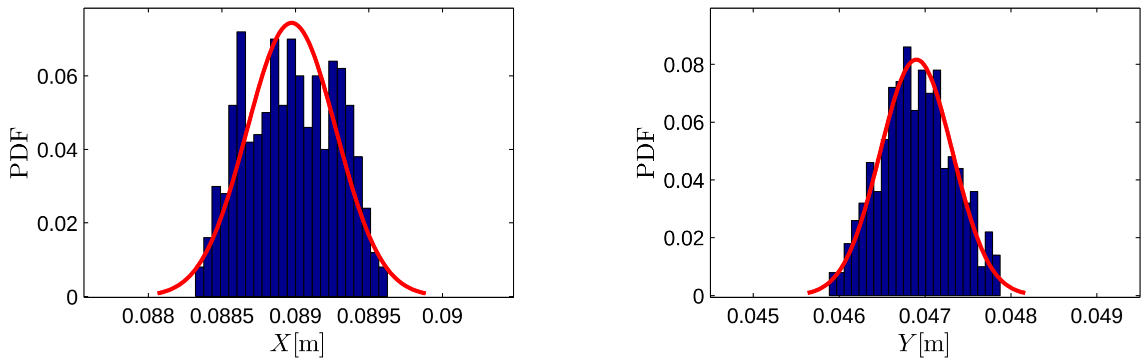

(a) $\mathcal{N}(\mu_x, \sigma_x^2)$. (b) $\mathcal{N}(\mu_y, \sigma_y^2)$.

Figure 7. Histogram and probability distribution function (PDF) for θ =30^o.

4. CONCLUSIONS

A numerical approach is presented to obtain the structure displacements that are produced by the stiffness of the structure and the joint clearances subject to uncertainties. The compliant displacement of the structure is obtained by a procedure from the matrix structural analysis (MSA). Additionally, the uncertainties of the parameters were modeled as random variables. The compliant displacements in the presence of the uncertainties affecting the clearances, inputs loads and joint stiffness were obtained by using the Monte Carlo Simulation.

The numerical results allowed to evaluate the effect of the joint clearance, input forces, and joint stiffness subject to uncertainty on the positioning accuracy of the mechanism. Based on the results, it is possible to estimate the statistical moments of the obtained structural displacement, and thus it was possible to estimate the probability density functions of the displacement.

Future work will consider the uncertainties on the stiffness of the links and also the experimental response of the mechanism will be compared to the numerical response to validate the proposed approach.

5. REFERENCES

Gonçalves, R.S., Carbone, G., Carvalho, J.C.M. and Ceccarelli, M., 2016. “A comparison of stiffness analysis methods for robotic systems”. *International journal of mechanics and control*, Vol. 17, No. 2, pp. 35–58.

Gonçalves, R.S. and Carvalho, J.C.M., 2009. "Stiffness analysis of parallel manipulator using matrix structural analysis". In *Proceedings of EUCOMES 08*, Springer, pp. 255–262.

Gonçalves, R.S., Carvalho, J.C.M., Carbone, G. and Ceccarelli, M., 2009. "A general approach for accuracy analysis of parallel manipulator with joint clearance". In *Proceedings of the 20th International Congress of Mechanical Engineering COBEM*.

Gonçalves, R., 2009. *Estudo De Rigidez De Cadeias Cinemáticas Fechadas. 2009. 239*. Ph.D. thesis, Universidade Federal de Uberlândia.

Gosselin, C., Angeles, J. *et al.*, 1990. "Singularity analysis of closed-loop kinematic chains." *IEEE transactions on robotics and automation*, Vol. 6, No. 3, pp. 281–290.

Júnior, G.S., Carvalho, J.C.M. and Gonçalves, R.S., 2016. "Stiffness analysis of multibody systems using matrix structural analysis–msa". *Robotica*, Vol. 34, No. 10, p. 2368.

Lara-Molina, F., Koroishi, E., Dumur, D. and Steffen Jr, V., 2015. "Stochastic analysis of a 6-dof fully parallel robot under uncertain parameters". *IFAC-PapersOnLine*, Vol. 48, No. 19, pp. 214–219.

Lara-Molina, F., Koroishi, E., Steffen, V. and Martins, L., 2018. "Kinematic performance of planar 5r symmetrical parallel mechanism subjected to clearances and uncertainties". *Journal of the Brazilian Society of Mechanical Sciences and Engineering*, Vol. 40, No. 4, pp. 1–15.

Lara-Molina, F.A. and Dumur, D., 2021. "A fuzzy approach for the kinematic reliability assessment of robotic manipulators". *Robotica*, pp. 1–15.

Lara-Molina, F.A. and Dumur, D., 2020. "Global performance criterion of robotic manipulator with clearances based on reliability". *Journal of the Brazilian Society of Mechanical Sciences and Engineering*, Vol. 42, No. 12, pp. 1–13.

Meng, J., Zhang, D. and Li, Z., 2009. "Accuracy analysis of parallel manipulators with joint clearance". *Journal of Mechanical Design*, Vol. 131, No. 1.

Montgomery, D.C. and Runger, G.C., 2010. *Applied statistics and probability for engineers*. John Wiley & Sons.

Pandey, M.D. and Zhang, X., 2012. "System reliability analysis of the robotic manipulator with random joint clearances". *Mechanism and Machine Theory*, Vol. 58, pp. 137–152.

Rao, S. and Bhatti, P., 2001. "Probabilistic approach to manipulator kinematics and dynamics". *Reliability Engineering & System Safety*, Vol. 72, No. 1, pp. 47–58.

Shabana, A.A., 2003. *Dynamics of multibody systems*. Cambridge university press.

Walz, N.P. and Hanss, M., 2013. "Fuzzy arithmetical analysis of multibody systems with uncertainties". *Archive of Mechanical Engineering*, Vol. 60, No. 1.

Zhang, X., Zhang, X. and Chen, Z., 2014. "Dynamic analysis of a 3-rrr parallel mechanism with multiple clearance joints". *Mechanism and Machine Theory*, Vol. 78, pp. 105–115.

6. RESPONSIBILITY NOTICE

The authors are solely responsible for the printed material included in this paper.